Optimizing the Preparation Procedure of Self-Assembled Monolayer of Stearic Acid for Protection of Cupronickel Alloy

Katarina Marušić,* Zana Hajdari and Helena Otmačić Ćurković

Faculty of Chemical Engineering and Technology, University of Zagreb, Marulićev trg 19, HR-10000 Zagreb, Croatia

* Corresponding author: E-mail: kmarusic@fkit.hr;
Tel.: +385 1 4597 163

***Paper based on a presentation at the 4th RSE-SEE 2013 Symposium
on Electrochemistry in Ljubljana, Slovenia***

Abstract

The aim of this work is to examine the possibility of CuNi protection in chloride media by self-assembled monolayers (SAMs) of stearic acid (SA). In order to obtain a compact, well ordered monolayer, that will provide long term protection, different SAM preparation procedures are studied. The influence of CuNi pretreatment, SA solution temperature and temperature of the drying period followed after the SA treatment on the protective properties of stearic acid self-assembled layer are examined by electrochemical methods and surface analysis techniques. The obtained results show that for complete self-assembled film formation it is necessary to have a drying period after exposing the sample to the stearic acid solution. Heating of the SA solution and drying period at higher temperatures result in layers with better stability in chloride media. The most compact surface layer, that provides long lasting and efficient protection to the underlying alloy, is obtained when prior to SA solution exposure an oxide layer on CuNi surface was formed at elevated temperatures.

1. Introduction

Application of self-assembled monolayers (SAMs) in corrosion protection of metals has raised a lot of interest recently.[1–9] Their protective effect is mainly explained by formation of a dense organic layer of well defined structure that blocks the active spots on the metal surface and presents a barrier to electron transfer and ion penetration. SAMs are well suited for this kind of application, as they are easy to prepare, do not require any specialized equipment for their preparation and can be constructed on objects of different sizes and shapes.[2] The advantage of such formed nanocoatings is that they can replace traditional corrosion inhibitors that are dissolved in corrosive media. In this way consumption of chemicals is reduced. This results in less expensive and more environment friendly protection.[3,4]

Organic compounds mostly used for preparation of SAMs on metallic surfaces are long chain alkanethiolates,[1,5,10] silanes,[1,9] phosphonic,[1,7,8,11] hydroxamic[1,3,4] or carboxylic acids.[1,2,6] While alkanethiolates bond with the bare metal surface,[5,10] other long chain compounds can adsorb on metallic oxides.[2,4,7–9,11,12] As most of the commercially important metals and alloys readily get covered by thin oxide layers when exposed to air, formation of SAMs on the oxide surface is interesting from a practical point of view.

Cupronickel alloys (CuNi) are often used in marine applications, e.g. for naval vessels, pipelines or desalination plants. Their good corrosion resistance in seawater results from the formation of a protective oxide film on the metal surface.[13] In order to prolong the service life time of cupronickel alloys different corrosion inhibitors may be applied, such as amino acids[14] or N,N-diethyldithiocarbamate salts.[15] Recent investigations have shown that SAMs of phosphonic acids provide efficient protection to cupronickel alloys in brine solutions.[7]

The aim of this work is to examine the possibility of CuNi protection in chloride media by SAMs of stearic

acid (SA). In literature it can be found that carboxylic acids form SAMs on oxide layers of stainless steel,[16,17] aluminium oxide[18–20] and copper oxide.[20] Their spontaneous adsorption can be considered as an acid-base reaction and the driving force is the formation of a surface salt between carboxylate anion and surface metal cation.[1]

By definition SAMs are easily obtained by immersion of a metallic substrate into a solution containing the surface-active compound. However, properties of such layers depend on preparation protocols including substrate cleaning, pretreatment, temperature, solution concentration, immersion time and drying procedure.

The intention of this work was to study the influence of several SAM preparation steps on its properties. In literature one can often find discrepancy between results of different research groups that are caused by differences in preparation protocols, mostly without explanation why such a procedure was used. [1,7,17]

In this paper we have examined the importance of two steps used in preparation of SAMs of organic acids on metal oxides: formation of an oxide layer that precedes the organic acid adsorption and drying as the last step in SAM formation. In literature one can find examples of preparation procedures that include both of these steps, only one, or even none (procedures with drying time of few seconds). Therefore, we believed that it would be interesting to study the role of each of the preparation steps. In this work influence of CuNi pretreatment, solution temperature and drying temperature on the protective properties of stearic acid monolayer are examined.

2. Experimental

2. 1. Sample Preparation

Investigations were performed on cupronickel alloy (Goodfellow Cambridge Ltd) with a composition given in Table 1. The specimens were cut-out from a cupronickel rod with a 1.3 cm diameter and 0.5 cm in thickness. In order to prepare working electrodes for electrochemical measurements on the back-side of these plates a copper wire was soldered, and then they were embedded into epoxy resin. The exposed surface of the working electrodes was 1.33 cm². The electrodes (or coupons for spectroscopic and contact angle measurements) were, prior to all investigations and/or surface treatment, abraded with emery paper grade 1000, 1500, 2000, and polished with α-Al$_2$O$_3$ particle size 0.1 μm, degreased with ethanol in ultrasonic bath and rinsed with re-distilled water.

Table 1. Composition of the cupronickel alloy.

Element	Cu	Ni	Mn	Fe
wt-%	67.3	31.0	1.0	0.7

A protective film on the surface of the alloy was prepared according to different procedures presented in Table 2. Initially, during oxide formation period, samples were either left in air for 24 h at room temperature or heated in furnace at 80 °C. Then the samples were immersed in stearic acid, CH$_3$(CH$_2$)$_{16}$CO$_2$H (SA) (Sigma-Aldrich

Table 2. The investigated SAM preparation procedures.

Oxide treatment (OT)	Oxide (OT) and SA treatment (SA)	Oxide (OT), SA treatment (SA) and drying (DRY)	
A (OT: 24h at 25 °C)	**B** (SA: 20h at 25 °C)	**C** (OT: 24h at 25 °C; SA: 20 h at 25 °C; DRY: 24 h at 25 °C)	Room temperature procedures (*RT procedures*)
D (OT: 24h at 25 °C, 3h at 50 °C)		**E** (OT: 24h at 25 °C; SA: 20h at 25 °C; DRY: 3 h at 50 °C) **F** (OT: 24h at 25 °C; SA: 20h at 40 °C; DRY: 5h at 50 °C) **G** (OT: 24h at 25 °C; SA: 1h at 40 °C; DRY: 5h at 50 °C)	Heat-treatments influencing the monolayer formation (*HM procedures*)
H (OT: 24h at 80 °C)		**I** (OT: 24h at 80 °C; SA: 20h at 40 °C ; DRY: 5h at 50 °C)	Heat-treatments influencing both the oxide film formation and monolayer formation (*HOM procedures*)

Chemie GmbH), diluted in ethanol at the concentration 0.01 mol/L at room temperature or at 40 °C (SA treatment). The electrodes were, after being emerged from the inhibitor solution, left to dry in air or in furnace (drying time). All the procedures can be divided into three groups: room temperature procedures (*RT procedures*), heat-treatments influencing the monolayer formation (*HM procedures*) and heat-treatments influencing both the oxide film formation and monolayer formation (*HOM procedures*).

2. 2. Electrochemical Investigations

Electrochemical investigations were conducted in a three electrode cell, in a solution simulating seawater, 3% NaCl. Platinum foil was used as counter electrode and saturated calomel electrode as reference electrode. All potentials in the text refer to the SCE scale. Prior to electrochemical measurements the electrodes were immersed in the test solution for 1 hour to stabilize the open circuit potential.

Electrochemical impedance spectroscopy was performed at E_{corr} in the frequency range 100 kHz – 10 mHz with a 10 mV rms amplitude. The wide (±150mV OCP) and narrow (±20mV OCP) potential range polarization were performed at potential scan rate of 0.166 mV/s. The electrochemical measurements were performed using a PAR 263A potentiostat / galvanostat and frequency response detector PAR 1025.

2. 3. Surface Layer Investigations

The contact angles on bare cupronickel and the SA treated samples were measured using a goniometer DataPhysics Contact Angle System OCA 20. Measurements were carried out with a drop of 1μL water under the ambient atmospheric conditions. The morphology of the cupronickel surface with and without SAMs was examined by a scanning electron microscope VEGA 3 SEM TESCAN at an acceleration voltage of 20 kV.

FTIR measurements were carried out by Perkin-Elmer Spectrum One. The scan range was 4000–650 cm^{-1} having a resolution of 0.5 cm^{-1}. The results were the averages of 4 scans.

3. Results and Discussion

3. 1. Short Time Exposure to the Sodium Chloride Solution

Samples that have been subjected to different treatments (listed in Table 2) have been examined after 1 hour exposure to the test solution by electrochemical impedance spectroscopy and potentiodynamic DC scan in wide and narrow potential range.

3. 1 .1. Monolayer Formation Treatments at Room Temperature (RT Procedures)

In the first part of our investigations treatments at room temperature were examined.

Figure 1 presents impedance spectra of samples that have undergone different treatments only at room temperature. In the following figures (Fig. 1–3) symbols represent experimental data and lines calculated data obtained by fitting the experimental data to the selected equivalent electrical circuits that will be explained in section 3.2. After polishing and degreasing, all samples were exposed to air for 24h at room temperature, in order to let a native oxide film form on the surface. This is the oxide formation period of the treatment. The oxide film is the metal's natural protecting system, and thus all treatments were performed to observe or enhance the performance of the oxide film.

- Sample A presents a sample that was not treated with SA and has only a native oxide film on the surface.
- Sample B was treated with SA at room temperature.
- Sample C was after SA treatment left exposed to air for another 24h prior to exposure to the 3% NaCl solution.
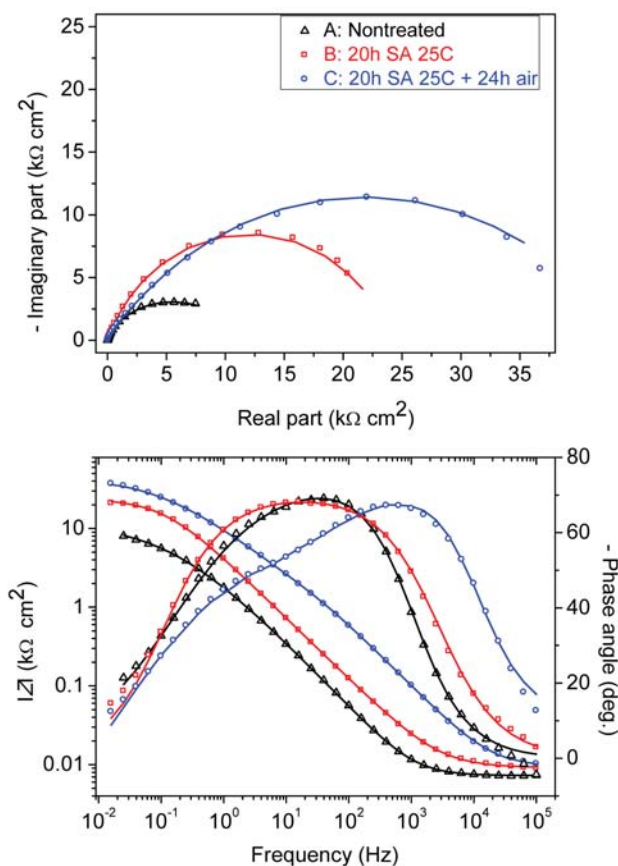

Figure 1. EIS spectra for samples prepared at room temperature: (a) Nyquist; (b) Bode plots.

It can be seen that when SA is present on the surface the impedance is significantly greater than in the case of the nontreated sample. While comparing samples B and C it can be seen in the Nyquist plot (Fig. 1(a)) that the impedance loop is similar in shape, but greater in the case of sample C.

In the Bode plot (Fig. 1(b)), a peak appears at 1 kHz in the phase angle plot of sample C which can be related to the formation of SAMs. Such a peak was not observed for sample B. This indicates that pure exposure of cupronickel to SA solution, at this concentration and immersion time, is not enough for a sufficiently protective layer to form. This period, when the metal is exposed to air (drying time), is needed to obtain a compact layer with good protective properties.

3. 1. 2. Heat-treatments Influencing the Monolayer Formation (HM Procedures)

After defining that for complete monolayer formation the metal needs to be left in air after exposing it to SA solution, influence of SA solution heating, as well as heating during the drying period on the SA layer properties was examined. Lower temperatures were chosen to avoid any chemical reactions or changes of the solution or SA layer.
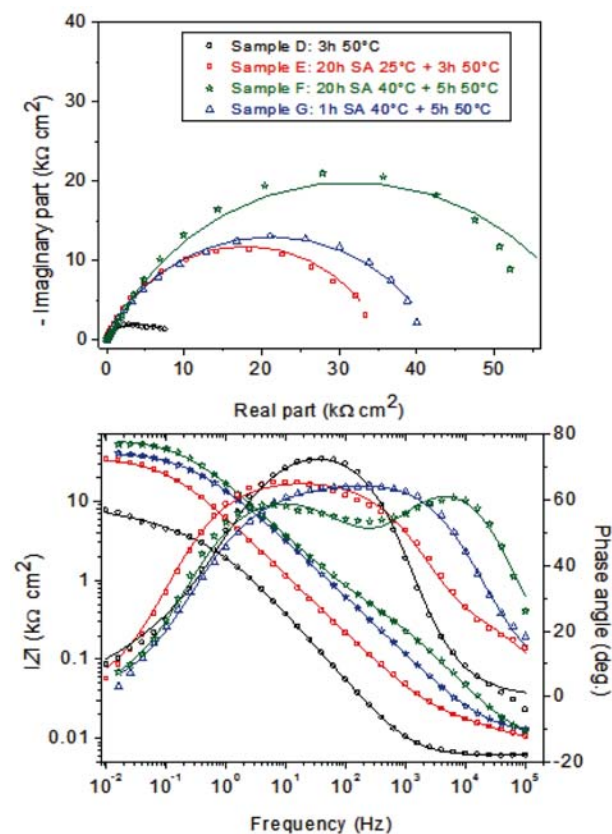

Figure 2. EIS spectra for samples that were heated during the monolayer formation period: (a) Nyquist; (b) Bode plots.

Figure 2 presents impedance spectra for the samples that have undergone following treatment:
– Sample D was not treated with SA, but heated in furnace for 3h at 50 °C.
– Sample E presents a sample that was after SA treatment at room temperature heated in furnace for 3h at 50 °C.
– In the case of sample F the SA solution was heated at 40 °C when cupronickel alloy was exposed to it. After SA exposure the sample was dried in furnace for 5h at 50 °C.
– Sample G was treated following the same procedure as sample F, but exposed to SA solution for only one hour.

It can be seen in Fig. 2a that heating of bare CuNi alloy (sample D) does not change significantly the impedance spectra compared to the sample that was just exposed to air (sample A). Similarly, sample E, that was after SA treatment at room temperature dried at 50 °C, exhibits absolute impedance at lowest frequencies (Fig. 2b) similar to that of sample C that was dried at room temperature (Fig. 1b). On the other hand, heating of SA solution results in increased impedance values (samples F and G). Actually, better results, ie. higher absolute impedance, were obtained for samples that were exposed for only one hour to the heated SA solution (sample G) than for the sample that was exposed to SA solution at room temperature for 24 hours. In Fig. 2b it can be distinguished that for all three SA treated samples two time constants appear, one at higher frequencies, related to the surface layer, and the second at lower frequencies, related to the corrosion reaction. Appearance of the time constant at higher frequencies indicates that in all three cases a protective layer is fully formed.

3. 1. 3. Heat-treatments Influencing Both the Oxide Film Formation and Monolayer Formation (HOM Procedures)

After investigating how heating affects the monolayer formation process, influence of the oxide formation procedure on the SA layer properties was examined. For that reason samples were heated for 24h at 80 °C before they were immersed in SA solution. Figure 3 presents EIS spectra of such prepared samples:
– Sample H was after polishing and degreasing treated in furnace for 24h at 80 °C.
– Sample I was after the same treatment exposed to SA solution at 40 °C for 20h and then again heat-treated in furnace at 50 °C for 5h.

It can be seen from Fig. 3 that the absolute impedance of sample H (Fig. 3b) does not differ significantly from samples A (Fig. 1b) and D (Fig. 2b) which were exposed to lower temperatures. However, when the SA layer was formed on a surface treated this way (sample I) it showed much higher impedance modulus than any of
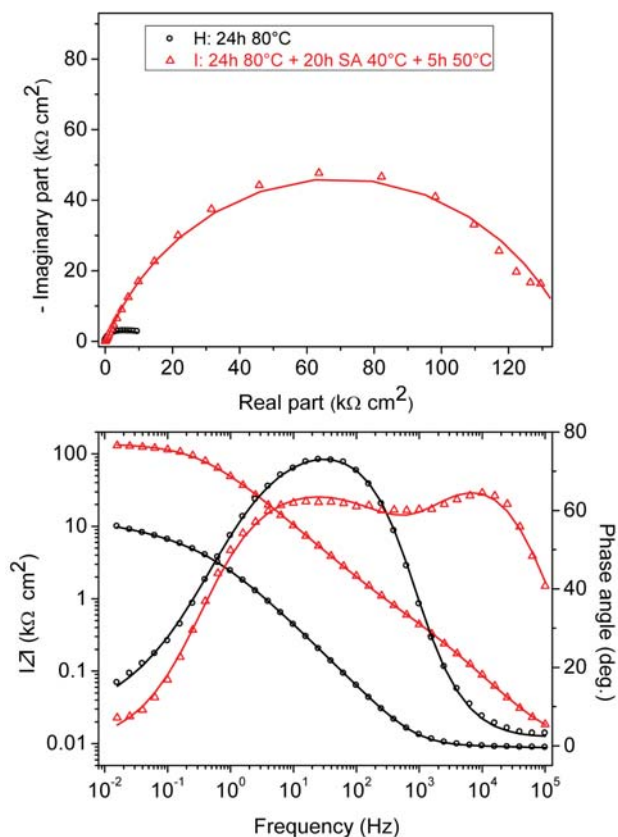
Figure 3. EIS spectra of samples heated during oxide formation period: (a) Nyquist; (b) Bode plots.

Figure 4. Polarization curves obtained in 3% NaCl.

the previous samples. This indicates that the oxide film formation procedure is important for the monolayer formation.

3. 1. 4. Overview of the Procedures

Figure 4 presents the results of the potentiodynamic DC scan in wide potential range (±150 mV) for samples with best results in the three groups of treatments and they are compared to sample A, the non-treated sample. Table 3 presents the corrosion parameters obtained from the polarization curve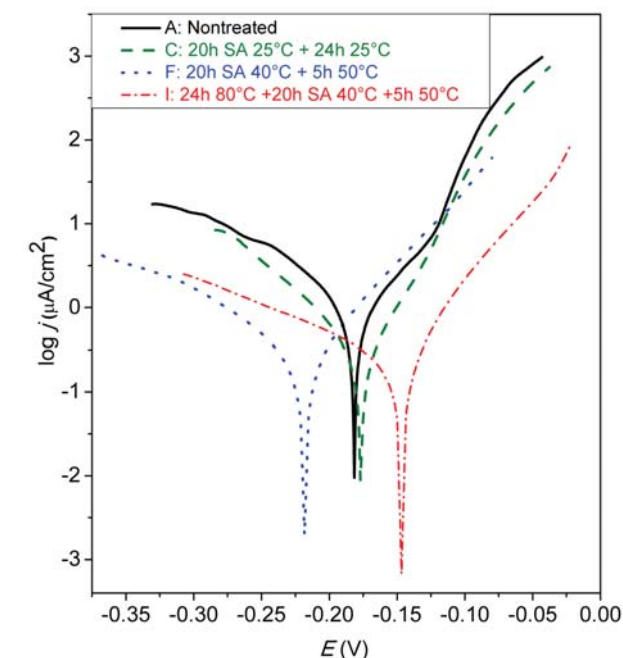s according to the Tafel extrapolation method: corrosion potential (E_{corr}), corrosion current density (j_{corr}), anodic and cathodic Tafel slopes (b_a and b_c).

It can be seen in Fig. 4 that in all three cases, when the SA layer is formed on the metal surface, the polarization curves are shifted towards the lower current densities compared to the non-treated sample. While in the case of sample C the polarization curve is shifted only slightly towards lower currents and its shape stays similar to the curve of the non-treated sample, the curves presenting samples F and I are shifted towards much lower currents. For sample F cathodic current densities have decreased greater than anodic current densities, while for sample I both anodic and cathodic current densities have strongly decreased compared to the nontreated sample.

Table 3 shows that the corrosion current densities are markedly smaller in all cases when SA is present on the surface. The corrosion inhibiting efficiency (*IE*) of each treatment is calculated according to following equation:

Table 3. Corrosion parameters obtained by Tafel extrapolation method.

Sample	E_{corr}, mV	b_a, mV · dec^{-1}	$-b_c$, mV · dec^{-1}	j_{corr}, µA · cm^{-2}	IE, %
A	–181.5	107	127	1.939	–
B	–195.1	51	94	0.384	80.2
C	–169.0	45	101	0.329	83.0
D	–198.0	46	81	0.834	56.7
E	–157.5	40	99	0.258	86.7
F	–214.2	51	93	0.205	89.4
G	–174.9	45	84	0.242	87.5
H	–169.9	45	85	0.512	73.6
I	–148.0	46	129	0.192	90.1

Table 4. Average polarization resistance, R_p, and standard deviation, σ.

Sample	R_p / kΩ cm^2	σ / kΩ cm^2
A	14.93	2.29
B	33.09	2.60
C	29.49	6.50
D	15.73	1.18
E	47.06	7.83
F	72.31	2.47
G	34.25	1.78
H	16.31	0.65
I	131.26	7.48

$$IE = \frac{j_{corr,0} - j_{corr,i}}{j_{corr,0}} \times 100\% \qquad (1)$$

The inhibiting efficiency of the SA layer is in all cases over 84 %, while for the sample I it is as high as 90.3 %.

The level of protection obtained by each SAM preparation procedure was also determined from the potentiodynamic DC scan in narrow potential range (±5 mV around the corrosion potential). From the reciprocal of the slope of the linear part of the polarization curve, polarization resistance, R_p (dE/dj), was determined. Table 4 presents the polarization resistance values after one hour of immersion in the 3% NaCl solution. It can be seen that the obtained values are very similar to the diameters of impedance loops of EIS spectra given in Figs. 1–3. These results confirm that the best protection is achieved when procedure I is followed. The standard deviation for each type of sample is also given in Table 4. It may be concluded that good reproducibility was achieved.

3. 2. Long Time Exposure to the Sodium Chloride Solution

Previously shown results examined the corrosion behaviour of differently prepared samples after 1 hour of exposure to the aggressive chloride solution. It is important to verify that the observed protection will remain over longer period of time. For this reason electrochemical measurements, potentiodynamic DC scan in narrow potential range (±20 mV) and electrochemical impedance spectroscopy, were performed during longer exposure times to the test solution.

Dependence of polarization resistance on exposure time to the corrosive media
Figure 5 presents the polarization resistance determined from the potentiodynamic DC scan experimental data collected in ±5 mV around the corrosion potential. Full lines present the RT treatments; dashed lines present the HM treatments; and the dotted lines present the HOM treatments.
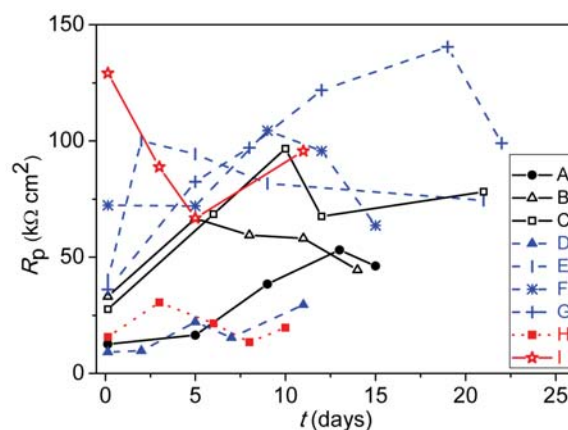
Figure 5. Polarization resistance as a function of immersion time in the sodium chloride solution.

As expected, the R_p values of the samples that are not covered with SA (A, D and H) are lower than of all the other samples. Sample A which was only polished shows the largest increase in R_p value after 5 days as a result of the growth of corrosion products. The native oxide layer on samples D and H offers somewhat better protection to the metal and thus this increase is smaller.

It can be seen that in most cases somewhere around the fifth day the R_p value takes a turn. Depending if SA is present on the surface it either starts increasing largely (corrosion products form) or it starts decreasing due to dissolution of the protective surface layer. In the case of samples C and F it takes around 10 days for this twist to take place.

After fifteen days of exposure to the NaCl solution only sample B, among all SA treated samples, has polarization resistance similar to that of the blank samples (A, D, H) while the other SA treated samples still exhibit superior polarization resistance.

Electrochemical impedance spectroscopy studies of corrosion protection stability
Electrochemical impedance spectroscopy was measured for each sample every few days for better understanding of the processes taking place on the metal's surface.

The impedance data of all the samples were fitted to equivalent electrical circuits presented in Fig. 6. They all consist of the electrolyte resistance between the working and reference electrodes, R_{el}, coupled with the R_{ct}-C_{dl} circuit which represents the corrosion reaction at the metal substrate/solution interface where R_{ct} is charge transfer resistance and C_{dl} is double layer capacitance. The equivalent electrical circuit containing only these elements is named 1RC and is given in Fig. 6a.

In case when a layer of SA or an oxide layer is present on the top of the metal surface, an additional time constant is observed at high frequencies that may be re-
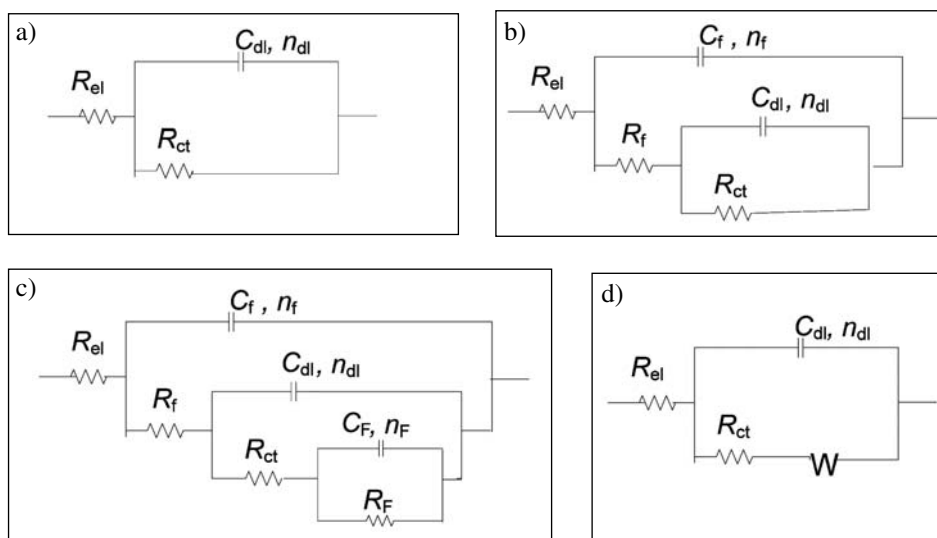
Figure 6. Equivalent electrical circuits used for fitting the EIS data: (a) 3*RC* circuit used for fitting sample A's data; (b) 1*RCW* circuit used for fitting sample B, D and H's data; (c) 2*RC* circuit used for fitting sample E, F, I and partially C's data; and (d) 1*RC* circuit used for fitting sample C's data.

presented by R_f-C_f couple where the R_f corresponds to the resistance due to an ionic flow and the C_f to the capacitance of the surface oxide or stearic acid film associated with the dielectric property of this film. This equivalent circuit is named 2RC (Fig. 6b). It was used for analysis of EIS data of all the samples that were covered by a SA layer, except sample C at longer immersion times.

Fig. 6c presents the 3*RC* circuit that was used to fit EIS data for sample A, the sample that did not undergo any kind of treatment. This is the only sample where corrosion takes place in such extent to form corrosion products on the surface in such quantity to be observed by an additional time constant. The R_F-C_F circuit is presented by faradaic resistance, R_F, and faradaic capacitance. These elements correspond to a redox process involving the corrosion products,[21] thus presenting properties of the corrosion products that form on the surface after long time exposure to corrosive media. For the capacitive loops, the coefficients n_f, n_{dl} and n_F are added to represent the depressed feature in Nyquist diagrams.

Fig. 6d presents the 1*RCW* circuit. In the cases where mass transport occurs in the corrosion reactions, i.e. diffusion, it creates impedance known as the Warburg impedance, which is presented with the Warburg element, *W*, coupled with the R_{ct}-C_{dl} circuit. Presence of Warburg impedance, i.e. diffusion, is commonly observed in impedance spectra of copper and CuNi alloys in seawater. In the case of pure copper appearance of Warburg impedance is explained by diffusion of soluble $CuCl_2^-$ from outer Helmholtz plane into the bulk solution,[22] while in the case of CuNi it is ascribed to oxygen diffusion in the pore electrolyte of porous layer of corrosion products.[23] In our experiments it occurs in the case of samples that do not have SA present on the surface (D and H), as well as of sample

B indicating poor corrosion protection of samples treated this way.

3. 2. 1. EIS Studies of the RT Treatments

The data obtained by fitting the EIS spectra of samples prepared at room temperature to electrical equivalent circuits given in Fig. 6. are presented in Fig. 7.

The nontreated sample A showed three capacitive loops. This is in accordance with the fact that above the oxide film, when the sample is not protected, a thick layer of corrosion products forms which is presented with its resistance R_F and capacitance, C_F. In the case of samples B and C the capacitive loop attributed to the layer of corrosion products was not observed indicating that the SA film, in both cases, slowed down the formation of corrosion products.

It can be seen in Fig. 7 that the R_{ct} increases for an order of magnitude when SA is present on the surface. The film resistance, R_f, that might be related to the existence of SA layer is observed only for sample C at the very beginning of exposure to the chloride solution. From these results it may be assumed that for sample B SA is adsorbed on active sites of the metal surface but no compact layer is formed. For sample C SA layer is formed but it is easily destroyed in the test solution, probably due to the presence of defects in the film that enable penetration of aggressive ions toward the metal surface.

3. 2. 2. EIS Studies of the HM Treatments

The impedance parameters obtained by fitting the EIS data to selected equivalent circuits are presented in Fig. 8 for the heat-treatments influencing the monolayer formation.
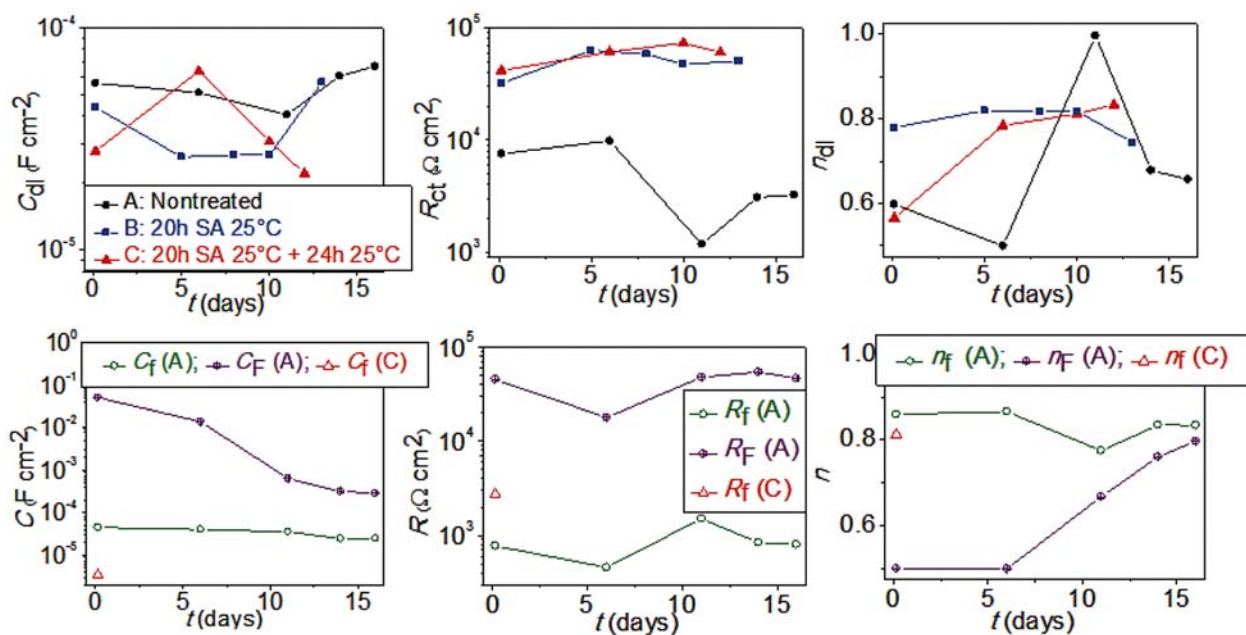
Figure 7. Fitted EIS data obtained for the RT samples.

The sample without SA present on the surface (sample D) was fitted to a 1*RCW* circuit. Compared with sample A the corrosion products film, represented with R_F-C_F circuit, was not observed. This indicates that heating the metal stimulates formation of a more compact oxide surface layer. Samples E and F exhibited two time constants for the whole immersion time, which indicates that the SA layer remains on the surface. This confirms that drying at elevated temperatures is a very important step towards the

formation of a stable layer of stearic acid. Similar observation was made by Raman and Gawalt[17] who found that the layers were formed but easily removed without an overnight annealing step.

As expected, R_{ct} is greater in the case of samples E and F and C_{dl} is clearly greater for sample D (Fig. 8).

At shorter immersion periods (see also Fig. 2), sample E showed lower corrosion resistance than sample F, which may be related to the difference in preparation pro-
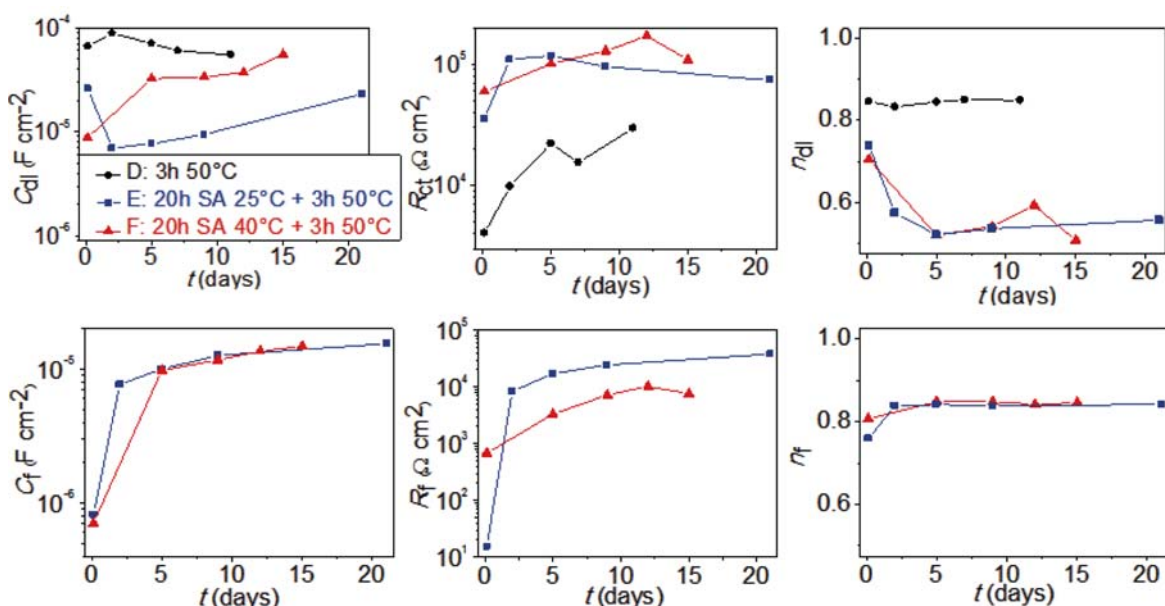

Figure 8. Fitted EIS data obtained for the HM samples.

cedure, ie. heating during SA treatment. At the beginning of immersion in the chloride solution a sharp change of C_f and R_f is observed for sample E and their values become similar to that of sample F. Later on there is no significant difference between the data for the two samples. In both cases the protection stays stable with time.

3. 2. 3. EIS studies of the HOM Treatments

The impedance parameters obtained by fitting the EIS spectra to the selected electrical equivalent circuits are presented in Fig. 9 for the heat-treatments influencing the oxide film formation.

As in the case of samples A and D Warburg impedance was observed on sample H and its impedance data were fitted to a $1RCW$ circuit (Fig. 6). The data of sample I were fitted to a $2RC$ circuit.

The R_f of sample I is in the beginning greater for an order of magnitude than for the samples E and F. In time it slightly decreases but stays rather high. This indicates that SA stabilizes and protects the oxide film formed according to the HOM treatment. Interestingly, both for samples E and F (Fig. 8) and sample I (Fig. 9) film capacitance C_f shows similar trend in time. Initial values of less than about 1 μF cm^{-2} (the lowest is for sample I) increase after the first few days of immersion and then remain constant with value of approximately 10 μF cm^{-2}. This increase in capacitance may be related to the penetration of water through the SA layer. Still, increase in capacitance is accompanied with increase in film resistance. The possible explanation for such behavior would be that because of water penetration down to the oxide layer the corrosion process occurs, which results in thicker and more protective oxide/SA surface layer.

3. 3. Surface Analysis

SEM, FTIR and goniometry were used to analyze the surface properties of differently treated samples.

Figure 10 presents the SEM images obtained on samples A, C, F and I. The samples were analyzed before and after exposure to NaCl for one week.

It can be seen on sample A that before exposure to NaCl the surface is relatively smooth, only with small cracks in the oxide layer that has formed on the cupronickel surface after exposing it to air for 24 hours. On sample C a SA leaf-like layer may be observed on part of the surface suggesting partial formation of nanoclusters rather than solely a monolayer. On the other hand, samples F and I have a more flat surface presumably due to thermal treatment that enhances chemical bonding of stearic acid to the oxide surface and results in formation of self-assembled monolayers that are too thin to be observed by SEM.

After a week in the NaCl solution the surface of sample A is covered by corrosion products. Sample C's surface is similar to sample A's. It is also covered by corrosion products but in a smaller extent than in the case of sample A. As for sample F, the surface layer is more uniform than for sample C, but there are still defects visible in the surface layer. Number of defects increases with exposure to NaCl. For sample I the surface layer seems much more compact after one week of exposure to NaCl. This is in good agreement with the fact that film resistance (R_f), obtained from impedance measurements, remains very high for the whole immersion period.

Contact angles of water were measured on selected samples. The results are presented in Table 4 and on Figure 11. They are in good agreement with those given in literature for SAMs of carboxylic acids on stainless steel[17] or on bronze.[6] The contact angle is significantly greater when SA is present (samples C, F and I) compared to when it is absent (samples A, D and H). The hydrophobic properties of the CuNi surface may be related to the CH$_3$-terminated SAM. The contact angle on these samples is slightly over 100° in all cases except for sample C. But in this case the deviation for sample C is much greater than for any other sample. This is in accordance with SEM analysis (Fig. 10) which showed that the surface layer on sample C has a partially flower like structure typical for highly hydrophobic surfaces.[6] It is quite interesting to notice that the most hydrophobic surface (sample C) did not show the highest corrosion resistance. The most probable explanation of this phenomenon is that without a drying period at higher temperatures a layer of stearic acid adhe-
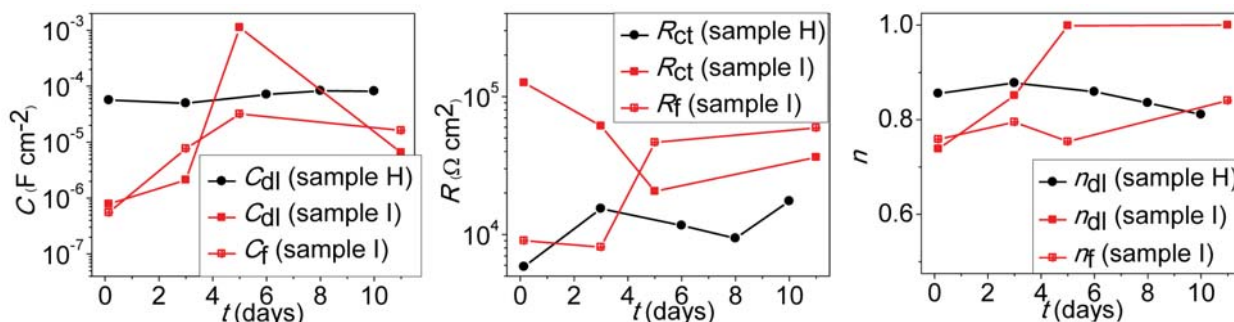

Figure 9. Fitted EIS data obtained for the HOM samples.

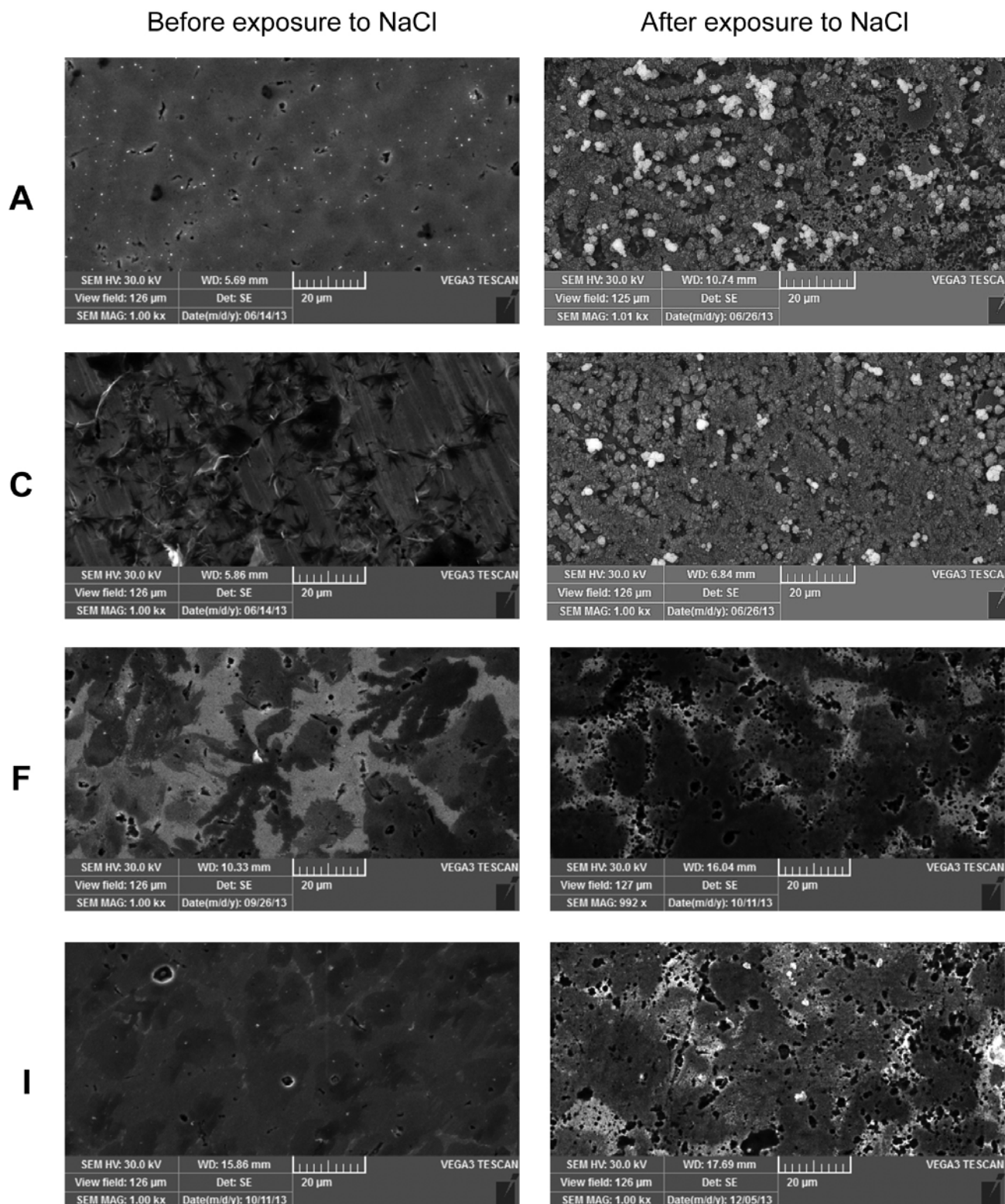Before exposure to NaCl After exposure to NaCl

**Figure 10.** SEM images of different samples.

res loosely to the metal surface and does not provide long term protection as observed from the results of electrochemical measurements.

Reports on layers of carboxylic acid with higher degree of hydrophobicity may also be found in literature, but they are mainly related to more complex self-assembled

Table 4. Contact angles of a drop of water on different samples

Sample	A	C	D	F	H	I
Contact angle, °	60±3	125±17	79±2	101±2	62±3	105±1

structures rather than monolayers. In literature one may find examples of nice flower-like hydrophobic structures of alkanoic acids formed on etched metal surfaces but with relatively low inhibiting efficiency towards corrosion due to weak adherence of the self-assembling structure to metal surface.[6] However, our aim was to obtain a compact monolayer of stearic acid, well adherent to metallic surface rather than a purely hydrophobic surface. As carboxylic acids are known to bind on metallic oxides, thermal oxidation of the metallic surface is an important step in SAM preparation.

a)

b)
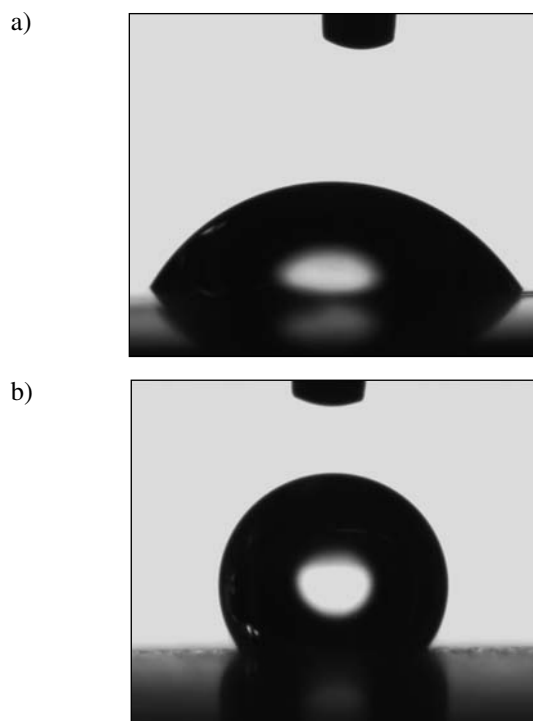
Figure 11. Contact angles of a drop of water on (a) sample A and (b) sample I.

The surfaces of the samples were analyzed by Fourier transform infrared spectroscopy. Figure 12 presents the results obtained on samples A, F and I. On sample C the same problem occurred as in the case of contact angle measurements, we obtained different spectra depending on the part of surface it was taken on. This is in accordance with SEM analysis which showed that sample C's surface is not uniform. As can be seen on Fig. 12 same spectrum was obtained on samples F and I.
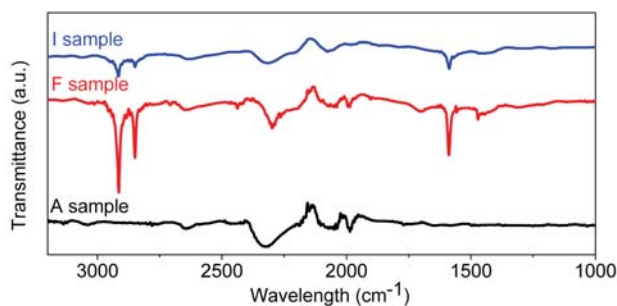
Figure 12. FTIR spectrum of samples A, F and I.

The FTIR spectrum of an "ordered" aliphatic monolayer is one with chains an all-trans configuration and it is characterized by $(v_{CH2})_{anti-sym} \sim 2918$ cm^{-1} and $(v_{CH2})_{sym} \sim 2849$ cm^{-1}.[17,24] Sample F formed well-ordered monolayers as both peaks were observed on it (2911 and 2855 cm^{-1}).

There are also peaks at 1589 and 1472 cm^{-1} for sample F. They correspond to carboxylate $(v_{COO^-})_{anti-sym}$ and $(v_{COO^-})_{sym}$ stretches. The peak corresponding to $v_{C=O}$ centred near 1700 cm^{-1} is not present. This indicates that the acid groups have become carboxylate groups and the monomers are bound to the surface in a bidentate fashion.[17]

4. Conclusions

In this work influence of several parameters of SAM preparation procedures on the protective properties stearic acid layers are examined. The results obtained by electrochemical methods show that in order to obtain a layer with good protective properties it is necessary to have a drying step after exposure of the sample to the stearic acid solution. If drying is preformed at higher temperatures (50 °C) the obtained layer has better protective properties than when drying is performed at room temperatures. Heating of the stearic acid solution has also positive effect on the layer stability. The highest corrosion resistance was obtained when prior to stearic acid solution exposure the oxide layer on CuNi surface was formed at 80 °C. In this case the most compact surface layer was obtained, as observed by SEM, which provides long lasting and efficient protection to the underlying alloy.

FTIR analysis have confirmed formation of a well ordered layer of stearic acid with the CH$_3$ group oriented towards the bulk solution which results in decrease of the surface wettability.

Contact angle measurements showed that surfaces of all the samples that have undergone stearic acid treatment were hydrophobic. However, the sample with the most hydrophobic surface did not exhibit the highest corrosion resistance. It was concluded that the drying procedure at higher temperatures may cause, on one hand, the

slight decrease in hydrophobicity, but on the other hand increase in stability of the stearic acid layer due to better adherence to the metal surface.

5. Acknowledgements

6. References

1. A. Ulman, *Chem. Rev.* **1996**, *96*, 1533–1554.
2. S. A. Jadhav, *Cent. Eur. J. Chem.* **2011**, *9*, 369–378.
3. J. Telegdi, T.Rigo, E. Kalman, *J. Electroanal. Chem.* **2005**, *582*, 191–20.
4. J. Telegdi, H. Otmačić Ćurković, K. Marušić, F. Al-Taher, E. Stupnišek-Lisac, E. Kalman, *Chem. Biochem. Eng. Q.* **2007**, *21*, 77–82.
5. G. Kane Jennings, P.E. Laibinis, *Colloids Surfaces A: Physiscochem. Eng. Aspects* **1996**, *116*, 105–114.
6. I. Milošev, T. Kosec, M. Bele, *J. Appl. Electrochem.* **2010**, *40*, 1317–1323.
7. K. M. Kruszewski, E. R. Renk, E. S. Gawalt, *Thin Solid Films* **2012**, *520*, 4326–4331.
8. G. Fonder, I. Minet, C. Volcke, S. Devillers, J. Delhalle, Z. Mekhalif, *Appl. Surf. Sci.* **2011**, *257*, 6300–6307.
9. A. Franquet, C. Le Pen, H. Terryn, J. Vereecken, *Electrochim. Acta* **2003**, *48*, 1245–1255.
10. R. G. Nuzzo, D.L. Allara, *J. Am. Chem. Soc.* **1983**, *105*, 4481–4483.
11. I. Milošev, M. Metikoš-Huković, Ž. Petrović, *Mater. Sci. Eng. C,* **2012**, *32*, 2604–2616.
12. A. Raman, R. Quinones, L. Barriger, R. Eastman, A. Parsi, E. S. Gawalt, *Langmuir*, **2010**, *26*, 1747–1754.
13. P. R. Roberge, Handbook of Corrosion Engineering, Mc-Graw-Hill, USA, **2000**, p.650.
14. Ghada M. Abd El-Hafez, Waheed A. Badawy, *Electrochim. Acta*, **2013**, *108*, 860–866.
15. M. Metikoš-Huković, R. Babić, I. Škugor, Z. Grubač, *Corros. Sci.* **2011**, *53*, 347–352.
16. G. Shustak, A. J. Domb, D.Mandler, *Langmuir*, **2004**, *20*, 7499–7506.
17. A. Raman, E. S. Gawalt, *Langmuir*, **2007**, *23*, 2284–2288.
18. K. M. Pertays, G. E. Thompson, M. R. Alexander, *Surf. Interface Anal.* **2004**, *36*, 1361–1366.
19. D. L. Allara, R. G. Nuzzo, *Langmuir*, **1985**, *1*, 45–52.
20. Y. T. Tao, *J. Am. Chem. Soc.* **1993**, *115*, 4350–4358.
21. K. Marušić, H. Otmačić-Ćurković, Š. Horvat-Kurbegović, H. Takenouti, E. Stupnišek-Lisac, *Electrochim. Acta* **2009**, 54, 7106–7113.
22. C. Deslouis, B. Tribollet, G. Mengoli, M. M. Musiani, *J. Appl. Electrochem.* **1988**, *18*, 384–393.
23. H. P. Hack, H. W. Pickering, *J. Electrochem. Soc.* **1991**, *138*, 690–695.
24. R. R. Sahoo, S. K. Biswas, *J. Colloid Interface Sci.* **2009**, 333, 707–718.

Povzetek

Cilj študije je raziskati možnost zaščite zlitine CuNi v kloridnem mediju s samourejenimi plasti stearinske kisline (SK). Z namenom priprave dolgoročne protikorozijske zaščite smo študirali različne načine tvorbe samourejenih plasti in sicer: predpripravo podlage CuNi, temperaturo raztopine SK in temperaturo sušenja po tvorbi plasti SK. Stopnjo zaščite smo preverili z elektrokemijskimi metodami in površinskoanaliznimi tehnikami. Za tvorbo plasti, ki omogoča visoko zaščito, je nujno samourejeno plast SK še sušiti na zraku. Segrevanje raztopine stearinske kisline pri višjih temperaturah izboljša stabilnost plasti v kloridni raztopini. Najbolj kompaktno plast SK, ki omogoča daljšo in učinkovito zaščito, smo dobili s predhodno tvorbo oksidne plasti na podlagi CuNi pri povišanih temperaturah.